

# AUTOMATIC SEGMENTATION OF SPINAL CORD IN MRI IMAGES VIA ITERATIVE CUCKOO SEARCH BASED RANDOM WALKER AND ONLINE KERNEL LEARNING (OKL) CLASSIFIER

Dr. D. Brindha, Assistant Professor, Department Of ECE, Coimbatore Institute of Engineering and Technology, Coimbatore.

N.R.Deepa, Assistant Professor, Department Of CSE, Coimbatore Institute of Engineering and Technology, Coimbatore.

Dr.Y.BabyKalpana, Associate Professor, Department of CSE, P.A.College of Engineering and Technology, Pollachi.

Dr.K. Murugan, Assistant Professor (Sr.G), Department of ECE, KPR Institute of Engineering and Technology, Coimbatore.

Dr.A.Devipriya, Assistant Professor, Department of CSE, KPR Institute of Engineering and Technology, Coimbatore.

**ABSTRACT:** Segmentation of Spinal Cord (SC) part has a major role in assessing spinal cord atrophy. Spinal Cord segmentation is not similar to that of brain segmentation, although Magnetic Resonance Imaging (MRI) sequence are greatly deployed for spinal cord examination. There is always a great challenge in spinal cord MRI segmentation which has been investigated by many researches. Also, considerable accuracy and degree of complexity for segmentation have been presented and elucidated in prevailing researches. A new approach namely combining Iterative Random-Walk (RW) solver and a Cuckoo Search Algorithm (CSA) has been suggested, thus facilitating direct homogenous and heterogeneous SC measurements comparison. An interactive RW solver with CSA is greatly utilized for complete cascaded pipelining in automatic manner. The initialization of automatic segmentation pipeline is done through powerful voxelwise classification via Online Kernel Learning (OKL) classifier. Therefore, SC topology refinement is done iteratively along with cascading of RW-CSA solvers for attaining proper segmentation outcomes in less iteration, even for cases including bone fractures and lesions. The segmentation experimental outcome mainly relies on MRI images indicating achievement of improved accuracy when compared with prevailing approaches.

**Keywords:** spinal cord segmentation, random walk algorithm, GLCM, OKL, MRI and cuckoo search algorithm

## 1. INTRODUCTION

Various neurological diseases study greatly necessitates examination of Spinal cord. In addition, segmentation and analysis methods in medical usage are not rapid and also labor-intensive at present particularly for pathological information. Spinal Cord is regarded as significant human part which helps in linking communication amid brain and various body parts. Also it is easily prone to traumatic spinal cord injury due to several ailments such as inflammatory diseases, infections, degenerative diseases and infections. An effectual clinical management critically demands accurate segmentation as well as spinal cord localization. Recently, imaging technology progression, precise internal organs structure as well tissues capturing can be done along with several diagnosis abnormalities on basis of scanned images. An unsupervised segmentation approach is suggested for spinal canal extraction in magnetic resonance (MR) images sagittal plane automatically. It does not require neither human intervention nor training for this segmentation method centered on a unusual saliency-driven attention model as well as standard active contour model

Many approaches has been proposed for capturing internal organs structure as well as tissues with good precision presently and exploited by physicians for diagnosing spine-related diseases on basis of computed tomography (CT) and magnetic resonance imaging (MRI). There exist few limitations in

assessing spinal cord on MRIs since it requires substantial user interaction or labor-intensive intervention for cord boundary perfect delineation, by which susceptibility increases for intra-rater and inter-rater variability, and labor intensive. Consequently, merely cervical cord single vertebral region is chiefly concentrated by several studies. Nevertheless, evidence from a recent post-mortem anticipates MS distresses various cord parts in a different way, besides consequently a larger region analysis is greatly benefitted [2].

Nuclear Magnetic Resonance (NMR) forms the basis for MRI system for mapping spatial location along with specific nuclei or protons properties in a subject by means of relations amid an electromagnetic field and nuclear spin [3]. Signals generated are detected in the course of placing hydrogen atoms in robust magnetic field besides agitating through resonant magnetic excitation pulse. Fat and water molecules are the main composition of human body. In addition, two hydrogen nuclei or protons two hydrogen nuclei or protons are comprised in each water molecule. Generally, hydrogen protons imaging is done for human tissues demonstration of physiological or pathological alterations.

In the course of MRI scanning, raw data found are intricate values representing Fourier transform of tissue volume magnetization distribution [4]. An inverse Fourier transform aids in transformation of raw data into magnitude, frequency and phase components which helps in physiological and morphological features representation for person actuality scanned. It is considered as zero mean uncorrelated Gaussian process with indistinguishable variance in both real and imaginary parts for noise in k-space in MR data from each coil. It happens due to Fourier transform linearity and orthogonality property. Nonetheless, transformation of complex valued images into magnitude and phase images occurs usually. A MR probability density function (PDF) changes due to non-linear operation takes place in magnitude (or phase) image calculation. Modelling of magnitude data in spatial domain is done as Rician distribution in single coil MRI systems which is termed as Rician noise (error amid important image intensities and measurement data) is locally signal dependent.

The main aim of Random walk is offering initial lesion detection on PET which might be deployed as object seed sets for PET and CT and additionally an initial shape model for tumors in CT images. The formulation of co-segmentation problem is regarded as energy minimization problem. Graph cut method performance is chiefly managed through energy function in graph based approach. A novel energy function is greatly utilized for PET and CT images characteristics adjustments. There are two terms namely region term and boundary term are involved in energy function of PET and CT segmentation. In addition, three components are encompassed in PET a cost based on SUV distribution, a downhill cost and a three-dimensional (3D) derivate function. Downhill cost is on the basis of tumor uptake analysis [5-6]. 3D derivative feature formulation is done using Hessian matrix combined with Gaussian functions. Shape constraint term integration into region cost function is done for CT. Consistent outcome amid PET and CT is obtained through context term aids in penalizing difference amid them which is then added to energy. Optimal solution pertaining to energy function minimization can be attained in a polynomial time through maximum flow computation in constructed graph. In this proposed methodology, the spinal cords segmentation is done in an automatic as well as iterative way. Automatic pipelining is initiated by new segmentation approach in which voxels in spinal cord MRI images are recognized. Voxels identification are greatly done which is of positive seeds by supervised Probability Boosting Tree (PBT) with Online Kernel Learning (OKL) Classification in addition to RW input and cuckoo search algorithm is utilized via cuckoo search algorithm.

## 2. LITERATURE REVIEW

Alizadeh et al [7] introduced an approach for precise as well as consistent spinal canal and spinal cord segmentation multi stage segmentation algorithm through multi stage segmentation algorithm which is obtained from contextual in pediatric spinal Diffusion Tensor MR Images. Initially, noise amplitude is alleviated and image homogeneity is enhanced through median filter and image compression approaches.

Subsequently, mathematical morphological processing application is utilized for segmenting besides regions labeling attributed to spinal canal. Segmented regions classification is done into spinal canal and background by Euclidean metric via segmented regions centroid coordinates in volumetric DTI data. Cord region extraction is applied by Otsu thresholding technique at last. The method is validated through examination of various performance metrics such as Segmentation accuracy, sensitivity, specificity and spatial overlap index along with quantitative measurements signifying approach effectiveness.

Kawahara et al [8] used an approach for obtaining spinal cord globally optimal segmentation through high dimensional minimal path search. Principal component analyses are greatly utilized for spinal cord cross-sectional shapes representation where maximal spinal cord's axial cross-sectional disparity and partial volume effects are captured. Variations to A\* minimal path search algorithm are utilized which rapidly mitigates necessitated memory and run-time for obtaining computational feasible high dimensional minimal path optimization. It is also revealed by volume agreement enhancement with expert segmentations besides a reduced amount of user interaction in contradiction with prevailing approaches.

Khan et al [9] elucidated about pattern existence in human spine degenerative process. Patients reassuring can be done by pattern unveiling so that their scan outcomes are not disease unusual or symptomatic. Various spinal features such as vertebral height, disc height, disc signal and para-spinal muscles are utilized for designing a model on basis of artificial neural networks. Aging impacts on lumbar spine features. Lumbar spine degenerative changes are considered into normal ageing process framework for patient "spinal age" assessment. A spinal growth in human being outline is explained by means of statistical features in this work. It greatly supports in obtaining a borderline amid normal, under and over growth of thumanspine pertaining to person's age.

Ling et al [10] describes a segmentation technique through 12-anatomical point representation (12-APR) scheme for human spine vertebra. The proposed method is a semi-automatic segmentation in which 12-points will be manually annotated on the region of interest (ROI) before automatic ROI extraction. The segmentation performance is evaluated using six performance metrics and outcomes reveal that recommended technique offers highest accuracy, specificity, Dice similarity coefficient, Jaccard similarity coefficient and cosine similarity coefficient.

In [11] Cuckoo Search Algorithm (CSA) is greatly utilized which is regarded as capable metaheuristic algorithm for solving various problems in many fields. Hill Climbing method is integrated with cuckoo search algorithm for establishing a new cuckoo search algorithm for obtaining solutions relating to integer and minimax optimization problems. The integration of the two algorithm is emerged as hybrid cuckoo search and hill climbing (CSAHC) which initiates searching through utilizing standard cuckoo search for many iterations, subsequently best-obtained solution is passed to hill climbing algorithm as an intensification process for accelerating search and mitigate standard cuckoo search algorithm slow convergence. The cuckoo search algorithm global exploration as well hill climbing method deep exploitation is primarily balanced by the algorithm 13 benchmarks are applied for performance validation through experimental simulations outcomes indicating improved performance for CSAHC when compared with standard CSA.

Zhang et al [12] attained image texture feature value extraction by utilizing GLCM and weight factor integration through direction measure for obtaining image final texture feature. Support Vector Machine (SVM) classifier combined with direction measure and gray level co-occurrence matrix fusion algorithm is mainly deployed for performing set of classification research for high-resolution remote sensing images. Classification outcomes are assessed through qualitative and quantitative methods. Improved image recognition is attained along with classification accuracy by texture feature extraction based on the fusion algorithm which is substantiated through experimental outcomes.

### 3. PROPOSED METHODOLOGY

A new approach namely combining Iterative Random-Walk (RW) solver and a Cuckoo Search Algorithm (CSA) has been suggested, thus facilitating direct homogenous and heterogeneous SC measurements comparison. An interactive RW solver with CSA is greatly utilized for complete cascaded pipelining in automatic manner. The initialization of automatic segmentation pipeline is done through powerful voxelwise classification via Online Kernel Learning (OKL) classifier. Therefore, SC topology refinement is done iteratively along with cascading of RW-CSA solvers for attaining proper segmentation outcomes in less iteration, even for patients including bone fractures and lesions. The segmentation experimental outcome mainly relies on MRI images indicating achievement of improved accuracy and robustness when compared with prevailing approaches. The following section explains the suggested MRI spinal cord segmentation methods in detailed manner.

Let us assume a set of  $n$  number of MRI scans as  $Images = \{Img_1, \dots, Img_n\}$ , and corresponding spinal cord segmentation  $Seg_i \in Seg$  in suggested MRI spinal cord segmentation problem.  $Img_i$  and  $Seg_i$  dimensions resembles the same. Every voxel in  $Seg_i$  is represented as  $v$  in segmentation process. Also, voxel probability is represented by  $q_v$  for foreground (spinal cord) and  $\bar{q}_v$  for background i.e. spinal cord outside, respectively. Once normalization is done, value of  $q_v + \bar{q}_v = 1$  respectively. A trivial set of foreground voxels along with high classification confidences are required for initiating spinal cord segmentation. Traditional spinal cord segmentation with reasonably low sensitivity but also low False Positives (FP) generation is done through these voxels which perform as positive seeds in Random walk (RW). The seed points are refined for improved spinal cord structure approximation by assuming all foreground voxels to be of continuous and smooth anatomic topology.

#### 3.1. Haar-Like Feature extraction

Haar-like features computation is attained from every sample voxel vicinity and thus signifying voxel local appearance. Particularly, 10 filter templates are greatly utilized for Haar-like features extraction from input MRI spinal cord image. One scale (i.e., 22 in voxels) and 11 translations along each axis are utilized for every filter template. Voxel wise classification is greatly achieved by these extracted Haar like features.

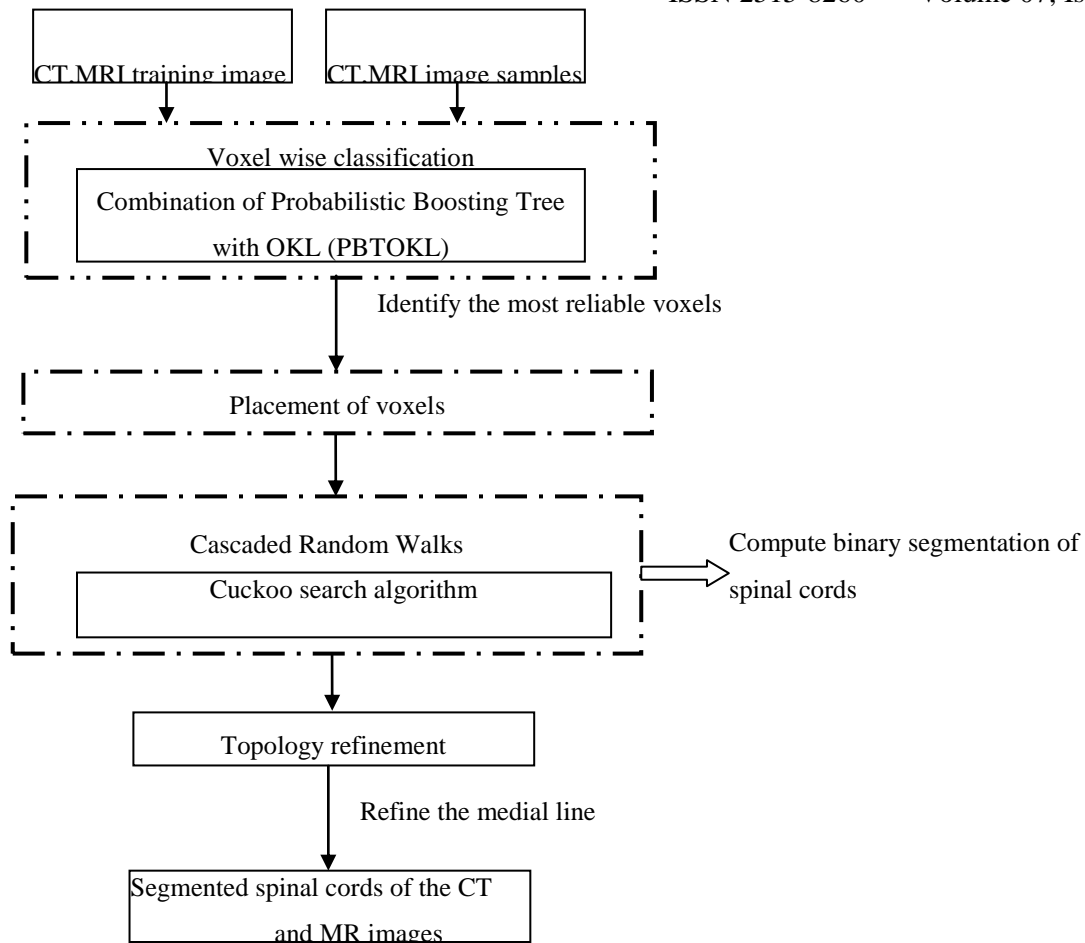


**Fig 1 Overall block diagram of suggested system**

### 3.2. Voxel wise classification with Online Kernel Learning (OKL) Classification

Online Kernel Learning (OKL) Classification is suggested for accomplishing voxel-wise classification problem. Let us assume an online binary classification task over a data instances sequence  $(x_t, y_t), t = 1, \dots, T$ , where  $(x_t \in R^d)$  notates t-th data instance observed features and  $y_t \in \{+1, -1\}$  represents true class label which is only revealed from environment at every online learning round end [13]. The main objective of traditional online kernel classification task is that learning a kernel-based predictive model  $f(x)$  for new instance classification  $x \in R^d$  as specified

$$f(x) = \sum_{i=1}^B \alpha_i k(x_i, x) \quad (1)$$

where B represents number of support vectors,  $\alpha_i$  signifies i-th support vector coefficient, and  $\kappa(\cdot, \cdot)$  represents kernel function. The prevailing budget online kernel classification methodology targets to bound number of support vectors through constant B using diverse budget maintenance schemes.

The goal is to construct a new representation  $z(x) \in R^D$  such that inner product has the ability for kernel function approximation:

$$R(x_i, x_j) \approx z(x_i)^T z(x_j) \quad (2)$$

Using above approximation, model can be reformulated:

$$f(x) = \sum_{i=1}^n \alpha_i k(x_i, x) \approx \sum_{i=1}^B \alpha_i z(x_i)^T z(x) = w^T z(x) \quad (3)$$

Where  $w^T = \sum_{i=1}^B \alpha_i z(x_i)$  indicates weight vector to be learned in t new feature space. Therefore, unraveling regular online kernel classification task might be changed into linear online classification task problem on new feature space resulting from kernel approximation. In this research, it presents the online kernel classification algorithm by using Fourier online gradient descent approach to improve the voxel wise classification more effectively.

In the Fourier online gradient descent method, random features are utilized in shift-invariant kernels. A shift invariant kernel is written as

$$k(x_1, x_2) = k(x_1 - x_2) = \int p(u) e^{iu^T(x_1 - x_2)} du \quad (4)$$

Where  $p(u)$  represents proper probability density function. Assume a kernel function to be continuous and positive-definite, based on Bochner's theorem, kernel function expression is given as a function expectation with a random variable  $u$ :

$$\int p(u) e^{iu^T(x_1 - x_2)} du = E_u[e^{iu^T x_1} \cdot e^{-iu^T x_2}] \quad (5)$$

In consequence, it can sample many random Fourier components  $u_1, \dots, u_D$  independently for new representation construction as follows:

$$z_t(x) = (\sin(u_1^T x), \cos(u_1^T x), \dots, \sin(u_D^T x), \cos(u_D^T x)) \quad (6)$$

The online kernel learning task approximation in original input space can therefore be done through solving a linear online learning task in new feature space. Further explicitly, for a Gaussian kernel

$k(x_1, x_2) = e^{-\frac{\|x_1 - x_2\|^2}{2\sigma^2}}$ , corresponding random Fourier component  $u$  with distribution  $p(u) = N(0, \sigma^{-2}I)$  may exist. For data arriving sequentially, new representation of a data instance on-the-fly can be constructed, besides performing online learning in new feature space via online gradient descent algorithm.

### Algorithm

**Input:** Number of Fourier components  $D$ , stepsize  $\eta$

Initialize  $w_1 = 0$

Generate random Fourier components:  $u_{1, \dots, u_D}$  sampled from distribution  $p(u) = N(0, \sigma^{-2}I)$

For  $t=1, 2, \dots, T$  do

Receive  $x_t$

Construct new representation:

$$z_t(x_t) = (\sin(u_1^T x_t), \cos(u_1^T x_t), \dots, \sin(u_D^T x_t), \cos(u_D^T x_t)) \quad (7)$$

Predict  $\hat{y}_t = \text{sgn}(w_t^T(z_t(x_t)))$

Receive  $y_t$  and suffer loss  $l(w_t^T(z_t(x_t)); y_t)$ ;

If  $l(w_t^T(z_t(x_t)); y_t) > 0$  then

$$w_{t+1} = w_t - \eta \nabla l(w_t^T(z_t(x_t)); y_t) \quad (8)$$

En if

End for

### Proposed Voxel-wise classification method

Voxel wise classification is greatly attained by online kernel learning algorithm which is involved for recognizing most consistent foreground i.e. Spinal cord voxels as positive seeds. MRI spinal cord image datasets is greatly utilized for voxel wise classification process. Voxels exactly along medial lines are sampled as foreground, whereas background candidates are acquired from a constant distance away to medial lines. Further, 3D Haar-like features are chiefly involved as voxel descriptors in suggested research. An abundant Haar-like features collection is proficiently calculated from each sample voxel neighborhood below consideration, consequently signifying voxel local appearance [13].

Once haar like features computation is done from 3D MRI spinal cord images, OKL method is adopted for Probabilistic Boosting Tree (PBT) training for voxel wise classification. As an alternative of using only one PBT classifier, a coarse-to-fine pyramid of PBT classifiers is constructed. Coarse features are exploited for PBT-based training/testing first, trailed by fine scales features. Also, coarse-scale features are deployed for reflecting longer range spatial context information in coarse resolution and generally restricted through traditional Haar filters. All image voxels classification as positive seeds is done through OKL with PBT classifiers while selecting Haar like features for segmentation error minimization. Every node in PBT signifies a new classifier using OKL with MRI images that reach PBT node. After classification two new child nodes are generated in PBT, as well as images are passed to children. Using this approach, MRI images that are difficult to classify can be classified with different Haar features than

those that are easy to classify. Since the purpose of voxelwise classification is to recognize extremely consistent foreground voxels merely. The foreground voxel confidence map with respect to a certain training image is revealed in Figure2. Nevertheless, as soon as OKL with PBT classifier is functional to a new testing image, classification outcome may suffer from both False-Negative (FN) and FP errors.

**Algorithm 1: Probabilistic Boosting Tree is combined with OKL classifier**

Given a training set  $S = \{(x_1, y_1, w_1), \dots, (x_m, y_m, w_m)\}; x_i \in \mathcal{X}, y_i \in \{1, \dots, n\}, \sum_i w_i = 1$

Compute the empirical distribution  $\hat{q}(y) = \sum_i w_i \delta(y_i = y)$

For each feature  $h_j$  at value  $v_j$  estimate the histogram  $his_{left}(k) = 1/z_{left} \sum_i \delta(k = y_i) w_i$  for  $y_i < v_j$  and  $his_{right}(k) = 1/z_{right} \sum_i \delta(k = y_i) w_i$  for  $y_i \geq v_j$

Determine the optimal  $h_j$  and  $v_j$  which attain the least entropy  $Z_{left} Entropy(his_{left}) + Z_{right} Entropy(his_{right})$

Create new set  $S' = \{(x_1, y'_1, w_1), \dots, (x_m, y'_m, w_m), x_i \in \mathcal{X}, y_i \in \{-1, +1\}\}$

Perform OKL classifier

Learning

$$L = \frac{1}{2} \|w\|^2 + C_{-1} \sum_{i \in S_{-1}} \xi_i + C_{+1} \sum_{i \in S_{+1}} \xi_i \quad (9)$$

Subject to  $y_i(w \cdot x_i) \geq 1 - \xi_i$

Where, the class label for pattern  $x_i$  is denoted by  $y_i \in \{-1, +1\}$ , the weight vector is represented by  $w$ , slack variables that allow margin failure is denoted by  $\xi_i$ , the set of patterns with class label -1 is indicated by  $S_{-1}$  and the associated penalty parameter representing a tradeoff within large margin and a small number of margin failures is denoted by  $C_{-1}$ .

Compute objective function

$$\text{Min} = \frac{1}{2} \sum_{i=1}^N \sum_{j=1}^N \alpha_i \alpha_j y_i y_j K(x_i, x_j) - \sum_{i=1}^N \alpha_i \quad (10)$$

The weight is expressed as

$$w = \sum_{i=1}^N \alpha_i y_i x_i \quad (11)$$

Decision function

$$f(x_p) = \sum_{i=1}^N \alpha_i y_i K(x_i, x_p) \quad (12)$$

$$\hat{y}(x_p) = \text{sgn}(f(x_p)) \quad (13)$$

$\hat{y}(x_p)$  is the predicted class label for pattern  $x_p$

Initially, the optimal feature is identified by this algorithm, through which the multi-class patterns are classified into two categories, and previous two-class boosting-tree algorithm is utilized to learn the classifiers. Remarkably, the boosting algorithm selects the first feature is same as the one which is selected after converting the multi-class into two-class, and the one selected for dividing multi-classes. In an intuitive manner, to take the robust decision, the first one is supported by the rest of the features/weak classifiers selected. In this way, the two-class classification problem turns out to be a special case of the multi-class classification issue. In accordance with the features, the identical objects belongs to various classes are united against others. Consequently, they are grouped in a gradual way, and set apart, since the expansion of tree continues. Once the classification of each class get accomplished, or in the scenario of lesser training samples, the expansion ends. Similar to the process carried out for the two-class problem is performed for multi-class PBT in terms of testing procedure. Once again, by integrating each probability from the sub-trees, a complete posterior probability is delivered by the top of the tree. With regard to the hierarchical structure of the multi-class PBT, it is considered being effective for computing the probability. This is significant at the time of recognizing numerous classes of objects that is considered being the problem of human vision systems which are dealing day-to-day. In the worst scenario, each tree node may be traversed. Nevertheless, it is rare case in practice.

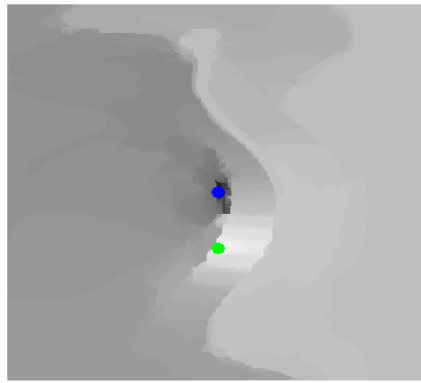


**Figure.2 shows the confidence map yielded by voxelwise classification on a training image**

### 3.2. Cuckoo Search (CS) algorithm for random walker

One of the biggest challenges of segmentation process involved in the existing segmentation approaches is addressed by the Random Walks (RW) segmentation algorithm [14], which is considered being a significant advantage of the algorithm. Being a voxel-wise graph-based system, the RW algorithm amounts to compute the probabilities of assignment of each voxel to each label (i.e. (e.g. the index of cords), when it gets utilized for segmenting the 3-D based MRI spinal cord images. During the process of this method, a large dataset segmentation system is solved to define and minimize the conventionality of the segmentation performed with the MRI image, which is measured by the energy function. Besides, this approach has the ability to segment huge volumes completely, since it includes efficient swarm intelligence based cuckoo search optimization algorithm for resolving such a problem. RW segmentation process annotates some voxels of each label in an automatic manner (the positive seeds in the proposed approach). Though it can provide significant time efficiency through evading automatic annotation of all voxels, yet this approach remains a time-consuming process as it automatically places the positive seeds, particularly in the scenario of segmenting the huge quantity of datasets. Like the PBT-based voxelwise classification, the RW solver also generates Voxel-wise probability of being foreground/background. Post specification of foreground/background seeds made by the users, the random-walk solver leaves from a specific non-seeding voxel, and its probabilities to attain foreground and background seeds have estimated as  $q_v$  and  $\bar{q}_v$ , respectively. Generally, the foreground is designated to non-seeding voxel  $v$  if  $q_v > \bar{q}_v$ . In the context of random walk, the MRI spinal cord image is embedded into a graph, during which edges link neighboring voxels, whereas vertices correspond to individual voxels. The following equation (15) expresses the estimation of likeness within two neighboring voxels, i.e.  $v$  and  $w$ .

$$WT_{vw} = \exp(-\alpha(Img_v - Img_w)^2) \quad (14)$$

In which, intensities at two locations have signified by  $Img_v$  and  $Img_w$ ; a positive constant has denoted by  $\alpha$ . Consider that the segmentation( $seg$ ) boundaries have perfectly aligned with intensity changes, then the random-walk solver tends to compute  $q_v$ , through which the subsequent energy function (11) is minimized.

$$E = \sum_{v \in v_w} WT_{vw}(q_v - q_w)^2 \quad (15)$$

In this method, optimization of aforementioned factor using CSA algorithm is similar to solving a region-based problem involved in MRI spinal cord images with boundary conditions, which have represented by the positive seeding voxels. Especially, **is set to 1 if is a foreground seed, and 0 for background**. The estimated incorporates spatial information across neighboring voxels are varies from the independent voxelwise classification.

Recently introduced algorithm called CS is known as a heuristic search algorithm [15-17], which is an inspiration of cuckoos' reproduction system. According to that, cuckoos lay the eggs in other host birds' nests that may belongs to different kind of species. If the host bird discover that the eggs are not belongs to

them, the eggs will be destroyed by the host bird or else it will abandon the nest. Consequently, the evolution of cuckoo eggs may mimic the eggs of local host birds.

- (1) Generally, one egg will be laid by cuckoo. Similarly, a set of solution will be coordinated at a time and it will get dumped in a random nest;
- (2) A fraction of the nests that possess the best eggs (solutions) will get carried over to the next generation;
- (3) Consider that the number of nests is static, and there is a probability that a host can discover an alien egg. Then, the host bird is able to either throw the egg or leave the nest and weave a new nest in another place.

In accordance with these 3 rules, the fundamental phases of CS are summarized in the form of pseudocode as given below,

1. Begin
2. Objective function  $f(x), x = (x_1, \dots, x_d)^T$
3. Generate initial population of n number of voxels  $x_i, (i = 1, 2, \dots, n)$
4. While e (t < MaxGeneration) //termination criterion
  - 4.1. Get a cuckoo randomly by Levy flights
  - 4.2. Evaluate the fitness of genes  $F_i$
  - 4.3. Compute objective function
  - 4.4. Find the more relevant voxels
  - 4.5. Choose the voxel (feature) among n (say  $x_i$ ) randomly
  - 4.6. If ( $F_{x_{i+1}} > F_{x_i}$ )
    - Replace  $x_i$  by the new voxel  $x_{i+1}$ ;
  - 4.7. Else
    - Keep voxel  $x_i$
  - 4.8. End if
  - 4.9. A fraction ( $p_a$ ) of worse genes are abandoned and new ones are built using below equation
 
$$x_i^{(t+1)} = x_i^{(t)} + \alpha \oplus Levy(\lambda) \quad (16)$$
  - 4.10. Keep the best voxels
  - 4.11. Rank the genes and find the current best
5. End while
6. Postprocess results and visualization
7. Update best voxel as optimal solution
8. End

As a vital component, the fitness energy function plays a significant role in CS algorithm. By utilizing the nest, the quality of segmentation method can be assessed through this method (segmentation accuracy of possible solution in MRI spinal cord image segmentation model). In Figure 2, foreground and background seeds that are utilized from the segmentation process are highlighted in green and blue, respectively. Besides, the random-walk solver alongside CS, and the segmentation approach are employed to estimate probability  $p_i$ . The segmentation results reveal that the segmented foreground inappropriately falls into two segment points that are disconnected.

In random walk, each voxel's probability  $q_i$  is correlated to the paths that connect the voxel and seeds. Apparently, it relies on the weights of the edges that form the path as well as the length of each path. Through this property, the random-walk solver can get weakened in a potential manner, through which the placement of the seeding voxels may get impacted.

**Random Walks:** This proposed approach is capable of identifying the seeds during voxel classification process and feeding them into RW with optimization CS algorithm for estimating segmentation. Generally, the initial segmented spinal cords break into numerous disconnected segments

that implicate high False Negative (FN) errors. Since the initial seeds with high self-assurance from voxelwise classification are usually not sufficient to cover positive seeds of the MRI spinal cords.

**Refinement Topology Process:** Through utilizing this proposed system, the overall segmentation in spinal cords is obtained and refined in order to accomplish the segmentation task in spinal cord MRI. Subsequently, the topology constraints of the MRI spinal cords to segmentation have introduced by this work. Its topology is specifically represented by using the medial line of the spinal cord. Post segmentation and calculation of each medial line of the spinal cord, the tentative segmentation is provided, and they are interleaved into a single connected curve.

There are two properties that need to be included in an interactive segmentation algorithm, i.e. i) The segmentation must not necessitate a surplus number of seeds, because they are directly proportional to the quantity of work necessitated by a user/the previous knowledge of a preprocessor, ii) It need not be over-reactive in terms of the placement of seeds inside an object.

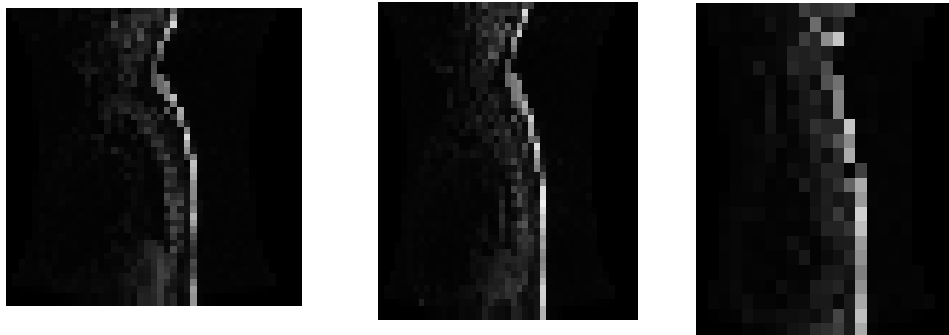
By using the following method, the sensitivity of each algorithm is evaluated on the basis of the number of seeds: Considering the first segmentation, the foreground is filled with foreground seed, and the background is filled with background seed. Subsequently, the seeds of both the foreground and background are eroded in a progressive way. Post-process of every erosion, re-computation of segmentation is done, and it is compared with the original segmentation. Once all the seeds belong to either foreground or background eliminated, the process ends. The seeds produced by this method predominantly look like skeletonization of the background/ object.

Throughout the iterative refinement process, the medial line is also permitted to grow at both ends of it, through which it gets enabled to accept the highly effective medial point. In this way, the results of RW for CS accompanied by refinement topology depict the efficiency of the proposed method to perform MRI spinal cord image segmentation. By using the RW segmentation technique, the proposed method proves its efficiency to improve the results of CSA.

#### 4. EXPERIMENTATION RESULTS

Considering the MRI spinal cord dataset, this research study evaluated the proposed techniques. Among the dataset used, 11 images have assigned for testing, and 36 images for training. The parameters, like Sensitivity, Specificity, precision and accuracy have considered during the evaluation of the proposed segmentation method. Whereas, 36 images have designated as testing and training data for the MRI spinal cord image segmentation that has carried out using DICOM dataset [18]. The results of the performance of newly introduced approaches have acquired through utilizing MATLAB.

**Performance Analysis:** Based on the parameters, such as sensitivity, specificity, precision and accuracy, the proposed segmentation method is scrutinized, during which 36 images have designated from the DICOM dataset as testing and training data for the MRI spinal cord image segmentation. Besides, the performance outcomes of the proposed methods have attained through MATLAB simulator. Considered parameters are given below:



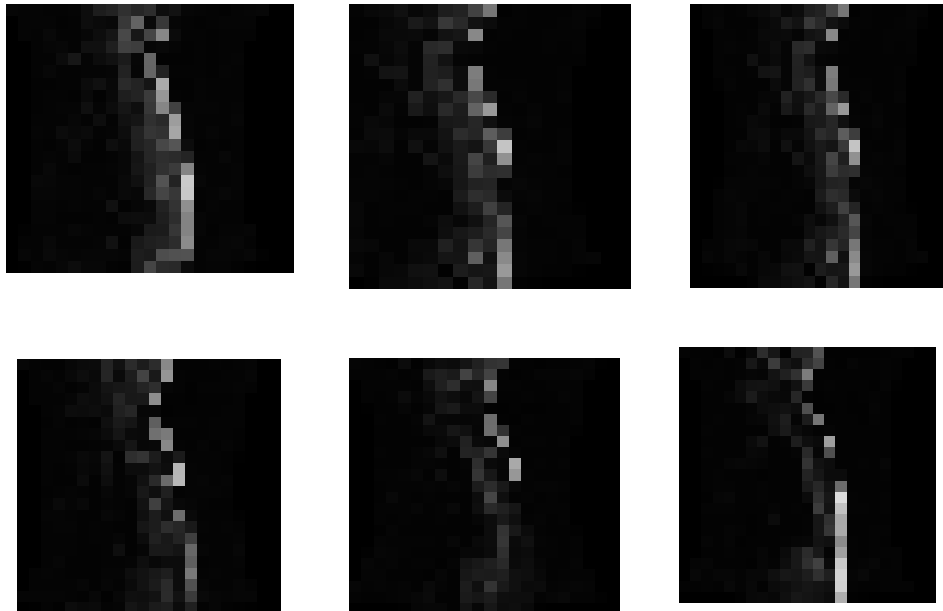


**Figure 3. Training MRI Spinal Cord Images used in the proposed Methodology**

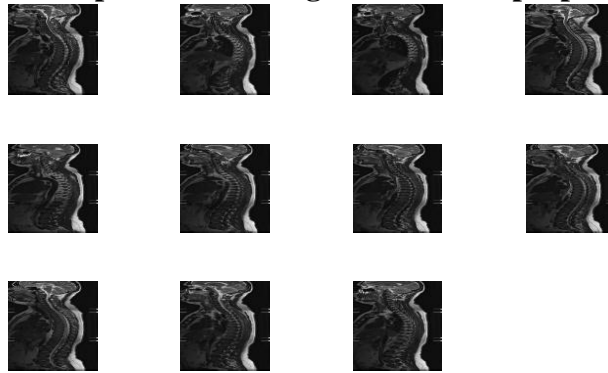


**Figure 4. Testing MRI Spinal Cord Images used in the proposed Methodology**

**Sensitivity (SN):** It referred to the True Positive Rate (TPR), which is also termed as recall. It represents the likelihood of correctly identified actual foreground through the classification process by employing SVM.

$$SN = \frac{TP}{(TP + FN)} * 100 \quad (17)$$

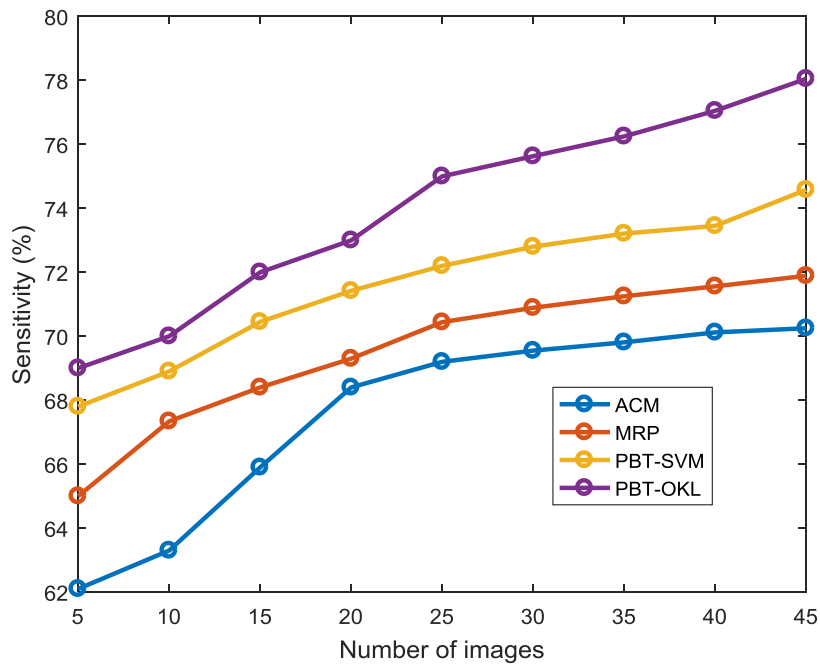


**Figure.5 Comparison results of the sensitivity using proposed and existing method**

Figure. 5 compares the results of the proposed PBT-OKL method, and the existing spinal cord segmentation techniques, like ACM, MRP, PBT-SVM in terms of sensitivity, where Y-axis stands for the sensitivity values, and the number of images lies on X-axis. From the graphs, the proposed PBT-OKL algorithms prove their adequacy to deliver 75% sensitivity rate that is 2.8% higher than PBT-SVM, 4.56% greater than MRP, and 5.8% higher than ACM approach, with regard to 25 images discussed in Table 1.

**Table.1. Sensitivity comparison results vs. SC segmentation methods**

Images	Sensitivity(%)			
	ACM	MRP	PBT-SVM	PBT-OKL
5	62.1	65	67.8	69
10	63.3	67.34	68.9	70
15	65.9	68.4	70.45	72
20	68.4	69.3	71.42	73
25	69.2	70.44	72.2	75
30	69.55	70.89	72.8	75.63
35	69.81	71.25	73.21	76.25
40	70.12	71.56	73.45	77.05
45	70.25	71.89	74.58	78.05

**Specificity (SP):** It defines the True Negative Rate, which indicates the probability of appropriately identified actual background.

$$SP = \frac{TN}{(TN + FP)} * 100 \quad (18)$$

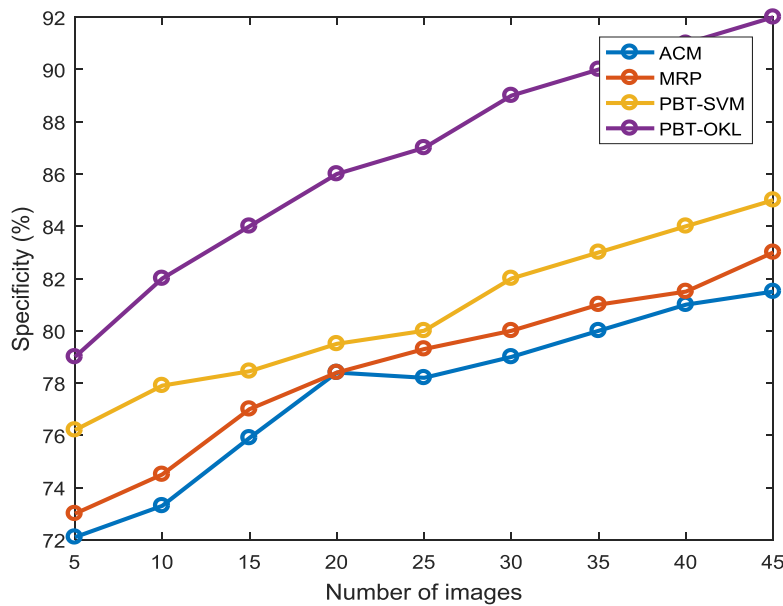


**Figure.6. Comparison results of the specificity using proposed and existing method**

In Figure 6, the specificity rates of the proposed PBT-OKL, and the existing ACM, MRP, and PBT-SVM methods for spinal cord segmentation have compared, in which Y-axis stands for the specificity values, and the number of images lies on X-axis. From the graphs, it is proved that the proposed PBT-OKL algorithms is efficient for delivering 87% specificity rate that is 7% higher than ACM, 7.7% greater than MRP, and 8.8% higher than PBT-SVM, with regard to 25 images discussed in Table 2.

**Table .2. Specificity comparison results vs. SC segmentation methods**

No.of images	Specificity (%)			
	ACM	MRP	PBT-SVM	PBT-OKL
5	72.1	73	76.2	79
10	73.3	74.5	77.9	82
15	75.9	77	78.45	84
20	78.4	78.4	79.5	86
25	78.2	79.3	80	87
30	79	80	82	89
35	80	81	83	90
40	81	81.5	84	91
45	81.5	83	85	92

**Precision(PR):** This parameter defines the probability of the relevance of foreground image that is randomly selected from the spinal cord images.

$$PR = TP / P = TP / (TP + FP) \quad (19)$$

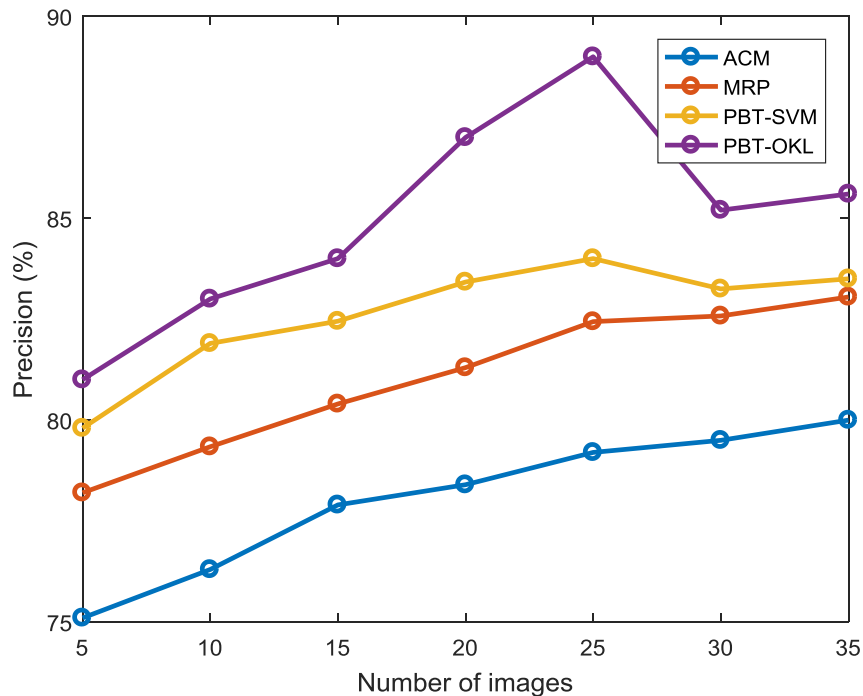


**Figure7 Comparison results of the precision using proposed and existing method**

Figure. 5 compares the results of the proposed PBT-OKL method, and the existing spinal cord segmentation techniques, like ACM, MRP, PBT-SVM in terms of Precision, where Y-axis stands for the precision results, and X-axis signifies the number of images. From the graphs, the proposed PBT-OKL algorithms prove their proficiency to provide 89% precision rate that is 5%, 6.56% and 9.8% higher than PBT-SVM, ACM, and MRP approaches, with regard to 25 images discussed in Table 3.

**Table .3. Precision comparison results vs. SC segmentation methods**

No.of images	Precision (%)			
	ACM	MRP	PBT-SVM	PBT-OKL
5	75.1	78.2	79.8	81
10	76.3	79.34	81.9	83
15	77.9	80.4	82.45	84
20	78.4	81.3	83.42	87
25	79.2	82.44	84	89
30	79.5	82.58	83.25	85.2
35	80	83.05	83.5	85.6
40	81.58	83.89	83.8	85.9
45	82	84.15	84.89	86.53

**Accuracy (A):** It refers to the ratio of the correctly classified foreground in the segmentation process, among the MRI spinal cord images as regards voxels.

$$A = \frac{(TP + TN)}{(TP + FN + FP + TN)} * 100 \quad (20)$$

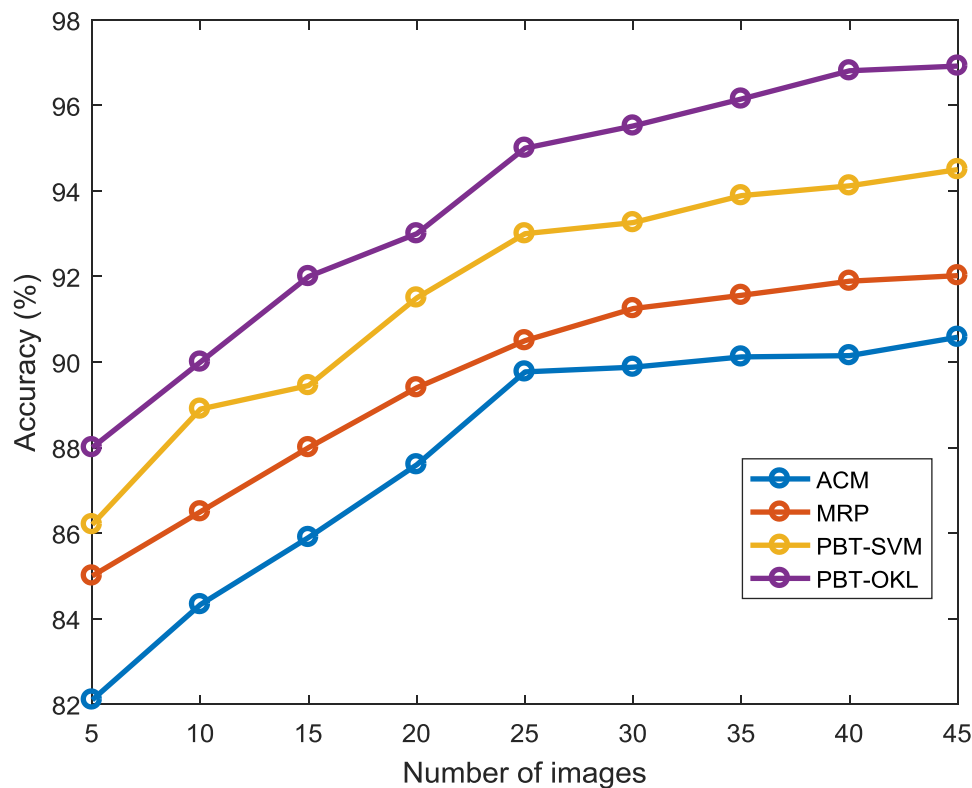


**Figure 8. Comparison results of the Segmentation Accuracy using proposed and existing method**

In Figure 8, the Accuracy rates of the proposed PBT-OKL, and the existing spinal cord segmentation methods, such as Active Contour Model (ACM), Multi-Resolution Propagation (MRP), PBT-SVM have compared, where Y-axis stands for the Accuracy rates, and X-axis represents the number of images. From the graphs, it is proved that the proposed PBT-OKL algorithms is efficient to provide 95% specificity rate that is 2% higher than PBT-SVM, 4.5% greater than ACM, and 5.23% higher than MRP methods, with regard to 25 images given in Table 4.

**Table 4. Accuracy comparison results vs. SC segmentation methods**

No.of images	Accuracy (%)			
	ACM	MRP	PBT-SVM	PBT-OKL
5	82.1	85	86.2	88
10	84.33	86.5	88.9	90
15	85.9	88	89.45	92
20	87.6	89.4	91.5	93
25	89.77	90.5	93	95
30	89.88	91.25	93.26	95.52
35	90.12	91.56	93.89	96.15
40	90.15	91.89	94.12	96.81
45	90.58	92.02	94.5	96.92

## 5. CONCLUSION AND FUTURE WORK

This research predominantly confers the segmentation of spinal cords from Magnetic Resonance Images (MRIs). Accordingly, feature extraction, Voxel-wise classification, and spinal cord interactive segmentation phases have significantly involved in this work. Initially, the highly consistent foreground has identified through carrying out Voxel-wise classification using PBT-OKL, during which the Spinal cord

voxels have considered as positive seeds. In the context of exactly sampling the voxels along with the medial lines as foreground, background candidates have derived from a constant distance away to the medial lines. Subsequently, the CS optimization algorithm has utilized to solve the new Random Walk (RW), and it has assigned to perform interactive segmentation. This function has iterated to make the cascading of various RW solvers possible and to construct the highly powerful model to segment the spinal cords from MRI images, even under multifaceted scenarios. When compared with MRP, ACM and PBT-SVM methods, the simulation outcomes depict that the proposed PBT with OKL classification approach is efficient for providing optimal accuracy. This indicates that the quality of MRI spinal cord segmentation is improved by the proposed PBT-OKL segmentation method by providing efficient voxels. This work tends to redefine the individual segments of the extracted medial line into a single one, for which homogeneous appearances have mainly focused for foreground voxels. Consequently, the detection of spinal cords on inhomogeneous image gets eased, through which the difference between homogenous and inhomogeneous regions has measured with the help of PBT with OKL. Ultimately, empirical findings prove the efficiency of the proposed PBT-OKL approach to deliver maximum rates of accuracy, specificity, sensitivity and precision that is higher than the existing methodologies.

## REFERENCES

1. Koh, Jaehan, et al. "An automatic segmentation method of the spinal canal from clinical MR images based on an attention model and an active contour model." *Biomedical Imaging: From Nano to Macro*, 2011 IEEE International Symposium on. IEEE, 2011.
2. Gilmore, Christopher P., et al. "Spinal cord atrophy in multiple sclerosis caused by white matter volume loss." *Archives of Neurology* 62.12 (2005): 1859-1862.
3. A.O. Rodriguez, Principles of magnetic resonance imaging, *Rev. Mex. Fis.* 50 (2004) 272–286.
4. Nyul, László G., Jayaram K. Udupa, and Xuan Zhang. "New variants of a method of MRI scale standardization." *IEEE transactions on medical imaging* 19.2 (2000): 143-150.
5. Ju, Wei, et al. "Random walk and graph cut for co-segmentation of lung tumor on PET-CT images." *IEEE Transactions on Image Processing* 24.12 (2015): 5854-5867.
6. C. P. Papageorgiou, M. Oren, and T. Poggio, "A general framework for object detection," in *Proc. 6th Int. Conf. Comput. Vis.*, 1998, pp. 555–562
7. Alizadeh, M., Mohamed, F.B., Faro, S.H., Shah, P., Middleton, D.M., Conklin, C.J. and Mulcahey, M.J., 2015, Segmentation of spinal cord in the pediatric spinal Diffusion Tensor MR Imaging. 41<sup>st</sup> Annual Northeast Biomedical Engineering Conference (NEBEC), pp. 1-2.
8. Kawahara, J., McIntosh, C., Tam, R. and Hamarneh, G., 2013, Globally optimal spinal cord segmentation using a minimal path in high dimensions. *IEEE 10<sup>th</sup> International Symposium on Biomedical Imaging (ISBI)*, pp. 848-851 .
9. Khan, A., Iliescu, D., Hines, E., Hutchinson, C. and Sneath, R., 2013, Neural Network Based Spinal Age Estimation Using Lumbar Spine Magnetic Resonance Images (MRI). 4<sup>th</sup> International Conference on Intelligent Systems Modelling & Simulation (ISMS), pp. 88-93.
10. Ling, C.S., Diyana, W.M., Zaki, W., Hussain, A. and Hamid, H.A., 2016, Semi-automated vertebral segmentation of human spine in MRI images. *International Conference on Advances in Electrical, Electronic and Systems Engineering (ICAEEES)*, pp. 120-124.
11. Basu, M. and Chowdhury, A., 2013. Cuckoo search algorithm for economic dispatch. *Energy*, 60, pp.99-108.
12. Zhang, X., Cui, J., Wang, W. and Lin, C., 2017. A study for texture feature extraction of high-resolution satellite images based on a direction measure and gray level co-occurrence matrix fusion algorithm. *Sensors*, 17(7), p.1474.
13. Desobry, Frédéric, Manuel Davy, and Christian Doncarli. "An online kernel change detection algorithm." *IEEE Transactions on Signal Processing* 53.8 (2005): 2961-2974.

14. Grady, L., 2006. Random walks for image segmentation. *IEEE transactions on pattern analysis and machine intelligence*, 28(11), pp.1768-1783.
15. Vo, D.N., Schegner, P. and Ongsakul, W., 2013. Cuckoo search algorithm for non-convex economic dispatch. *IET Generation, Transmission & Distribution*, 7(6), pp.645-654.
16. Manikandan, P. and Selvarajan, S., 2014. Data clustering using cuckoo search algorithm (CSA). In *Proceedings of the Second International Conference on Soft Computing for Problem Solving (SocProS 2012)*, December 28-30, 2012 (pp. 1275-1283). Springer, New Delhi.
17. El-Fergany, A.A. and Abdelaziz, A.Y., 2014. Capacitor allocations in radial distribution networks using cuckoo search algorithm. *IET Generation, Transmission & Distribution*, 8(2), pp.223-232.
18. Spine MR Image from the website: <http://www.osirix-viewer.com/datasets/>